CRYSTAL GROWTH & DESIGN
2002
VOL. 2, NO. 6
553−562

Quinoline Binding Site on Malaria Pigment Crystal: A Rational Pathway for Antimalaria Drug Design

Ronit Buller,*,† Matthew L. Peterson,‡ Örn Almarsson,‡ and Leslie Leiserowitz*,†

Department of Materials and Interfaces, The Weizmann Institute of Science, Rehovot 76100, Israel, and Transform Pharmaceuticals Inc., 29 Hartwell Avenue, Lexington, Massachusetts 02421 USA

Received July 2, 2002

ABSTRACT: Human malaria, one of the most striking, reemerging infectious diseases, is caused by several types of *Plasmodium* parasites. As the parasite digests hemoglobin in human red blood cells, the heme byproduct crystallizes into micron-sized malaria-pigment (hemozoin). Making use of a recently reported powder-crystal structure determination of synthetic hemozoin (β-hematin), we describe here its theoretical growth form and show it to be similar in habit and form to that of natural hemozoin. With this information, we propose a noncovalent binding site for the quinoline drug family at the end face of the fastest-growing direction of β-hematin. This adsorption mechanism is examined in terms of crystal growth inhibition vis-à-vis published data. The surface binding site elucidates the difference in activity of various quinolines, revealing the importance of the different quinoline functionalities. The interplay between molecular chirality of quinolines and the chirality of centrosymmetric β-hematin crystal faces is analyzed in terms of crystal growth inhibition. We additionally propose a molecular isomerism of the crystalline building blocks, with implications on quinoline surface binding, as well as on nucleation and size of β-hematin crystals.

Introduction

Although once considered an eradicated disease, malaria has reemerged rapidly mainly due to parasitic resistance to commonly used antimalarial drugs. Once again, malaria has become one of the most striking and widespread infectious diseases. There are some 300−500 million cases resulting in 1−3 million deaths per year, mostly of which are children under the age of five.[1]

Humans are affected by four protozoa parasite types of the genus *Plasmodium*: *vivax*, *ovale*, *malariae*, and *falciparum*. Of these, *falciparum* is the most virulent. The life cycle of the parasite is complex and incompletely understood. During the course of its life cycle, the parasite resides in several cells in both human-host and mosquito-vector, at various developmental stages and forms. One of the most extensively studied is the red blood cell (RBC) stage.[2] However, despite the impact of malaria on worldwide public health, neither the mechanism by which the parasite digests hemoglobin from mature RBCs, nor the action of the current antimalarial drugs are fully understood.[3,4]

Like most living organisms, malaria parasites require amino acids and the presence of iron, both of which can be obtained from hemoglobin. The parasite can digest up to 75% of the RBCs content, in a process, whereby the globin is enzymatically cleaved into small peptides, producing free heme (Fe^{2+}- protoporphyrin IX: Fe^{2+}-PPIX) as a byproduct. The toxic heme is rendered less harmful in the parasite by one electron oxidation to produce hematin (Fe^{3+}-PPIX), which then precipitates forming nonreactive submicron to micron-sized crystals known as hemozoin, in an exclusive organelle—the acidic food vacuole.[3,5] Hemozoin, the malaria pigment, is a marker of malaria infection in RBC assays. This process of hemozoin formation is now being considered[4,6,7] as a type of biomineralization.[8]

Malaria reemerged mainly as a consequence of developing parasite resistance. This resistance to quinoline-based drugs, which are the widest used, prevents the drug from accumulating in the food vacuole,[9] the location of the target site.[10] Leading proposals for the mechanism of resistance include changes in the transmembrane quinoline-drug flux in either the cytoplasmic or food-vacuole parasitic membranes, or pH alteration within the food vacuole.

For half a century, chloroquine was extensively used as the major antimalarial throughout the world, affecting the RBC stage of the parasite. Chloroquine is a synthetic analogue of the oldest known antimalarial, quinine. It is clinically more effective than quinine, as well as being inexpensive. As a base of $pK_{a1} = 8.1$, $pK_{a2} = 10.2$, chloroquine is partially uncharged at the natural body pH, enabling its passive transport through cell membranes.[11−13] Inside the acidic food vacuole of the *plasmodium* parasite ($pH = 4.8 \pm 0.4$), the drug becomes doubly protonated,[14] mostly accounting for its selective accumulation within the vacuole up to millimolar concentration.[15−20] Extensive usage of the drug and surging resistance have stimulated development of other effective quinoline analogues[21,22] that incorporate the bicyclic quinoline skeleton, and a flexible amine moiety at site C4 (see Scheme 1b (i) for atomic numbering).

The interaction of quinolines with hematin has been well established and studied over the years, and was initially proposed in 1967 by Macomer et al. for chloroquine.[23] Two main routes have been invoked to account for the primary mode of action of the quinolines: complexation with hematin in solution[22] and inhibition of malaria-pigment growth by quinoline attachment to the growing crystal.[6,24,25] Both models

* Corresponding authors: The Weizmann Institute of Science, Rehovot 76100, Israel, Phone: 972−8−934−3727, fax: 972−8−934−4138, e-mail: ronith.buller@weizmann.ac.il, leslie.leiserowitz@weizmann.ac.il.
† The Weizmann Institute of Science.
‡ Transform Pharmaceuticals Inc.

10.1021/cg025550i CCC: $22.00
Published on Web 08/27/2002

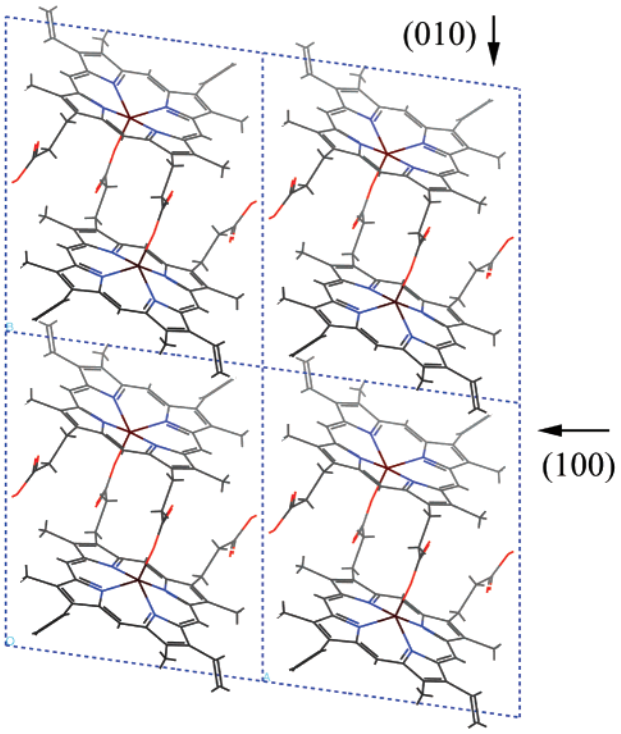

Figure 1. Packing arrangement of β-hematin viewed along the *c*-axis. Some (*h*,*k*,*l*) planes are indicated.

concur regarding the noncovalent nature of the interaction between drug and its target.

In a recent landmark study, Pagola et al.[20] determined the crystal structure of synthetic β-hematin by X-ray powder diffraction of micron-sized crystals using synchrotron radiation. β-Hematin is chemically, spectroscopically, and crystallographically identical to the malaria pigment hemozoin. The authors showed that the crystal structure[26] (Figure 1) is composed of hematin molecular units linked through iron−carboxylate bonds into centrosymmetric cyclic dimers, not polymer strands as had been originally believed. On the basis of this crystal structure determination and the low concentration of the drug in the blood stream, the authors have proposed that the quinoline antimalarials act through growth inhibition of hemozoin crystals as a result of absorption onto its actively growing faces. This prediction is reinforced by in vitro experiments,[4,21,22,24,27−29] using incubation of hemozoin crystals and its analogues with various quinolines, in which the quinoline family was found to retard the crystal growth. Experiments[24] show that extraction of the bound drug is achievable by either successive washing, or quinoline−drug competition.

We have determined the theoretical growth form of β-hematin, and show that it is similar in habit (i.e., overall shape) and form (i.e., *h*,*k*,*l* type of faces) to that of malaria pigment crystals. With this information in hand, we propose a noncovalent binding site for the quinoline family at the end face of the fastest-growing direction of the β-hematin theoretical form, as well as potential binding sites on other crystal faces, and examine the adsorption mechanism in terms of crystal growth inhibition vis-à-vis published experimental data. The proposed binding site clarifies the differences in activity of various quinolines and also reveals the role played by their functional groups in binding to the hemozoin surface. We further propose a molecular isomerism of the β-hematin cyclic dimer, with implication on the binding of quinolines to β-hematin crystal surface, as well as on the nucleation and size of β-hematin crystals.

Table 1. Crystal {*h*,*k*,*l*} Face Attachment Energies E_{att} (in kcal/mol) of β-Hematin Calculated for Determination of the Theoretical Growth Form (Figure 2a,b)[a]

face	E_{att} [kcal/mol]	face	E_{att} [kcal/mol]	face	E_{att} [kcal/mol]	face	E_{att} [kcal/mol]
{100}	−30.6	{110}	−52.6	{$\bar{1}$11}	−80.4	{$\bar{1}$21}	−106.8
{010}	−27.7	{011}	−82.4	{1$\bar{1}$1}	−92.8	{112}	−112.6
{001}	−101.5	{1$\bar{1}$0}	−52.9	{11$\bar{1}$}	−112.1		
		{10$\bar{1}$}	−108.1				

[a] The crystal faces formed are {100}, {010}, {011}, and {001}.

Results and Discussion

Theoretical Growth Form of β-Hematin and Comparison with Hemozoin. The morphology of the micron-sized crystals of β-hematin and of various malaria pigment crystals has yet to be experimentally described in terms of the crystal unit cell axes. The morphology of a crystal is determined by the relative growth rates of its various faces, the general rule being that faces that grow slowest are expressed in the crystal habit. The basic rules for a quantitative determination of crystal morphology as determined by the crystal structure only were laid down by Hartman and Perdok[30−32] and Hartman and Bennema:[33] The crucial relation is between the layer energy, E_l, the energy released when a layer is formed, and the attachment energy, E_{att}, the energy per molecule released when a new layer is attached to the crystal face. E_{att} controls the growth rate perpendicular to the layer, whereas E_l measures the stability of the layer. The morphological importance of a crystal face is inversely proportional to its attachment energy. The energies E_l and E_{att} may be computed using atom−atom potential energy functions. By applying such a procedure it became possible to calculate the energy values of E_l and E_{att} for various low-index faces of crystal, from which the "theoretical crystal form" may be derived. This method has been applied for a variety of organic[34−38] and inorganic[39] crystals. It is important to note that solvent and additives can dramatically affect the crystal habit, as well as the type of faces expressed.[40,41]

The computed crystal attachment energies E_{att} (Table 1) yielded the theoretical growth form of β-hematin (Figure 2a,b), making use of the Cerius2 software package.[42] The crystal morphology is needlelike, extended along the *c*-axis, exhibiting dominant {1,0,0} and {0,1,0} side faces, a less-developed {0,1,1} and a minor {0,0,1} face.[43] Faces of the type {*h*,*k*,*l*}, where *h*, *k*, and *l* are nonzero, are not formed since they have very negative attachment energies (Table 1), in keeping with the highly corrugated nature of such faces. By a similar criterion the {*h*,*k*,0} faces, such as {±1,1,0} are not manifest, being corrugated as is evident from the crystal structure (Figure 1), and thus with attachment energies larger than for either {1,0,0} or {0,1,0} (Table 1).

The theoretical morphology (Figure 2a,b) appears to be very similar in both habit and form to that of the

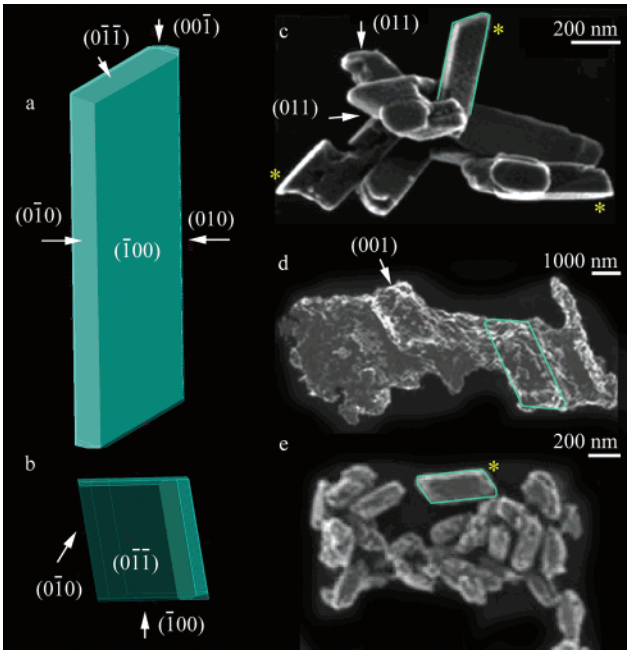

Figure 2. (a, b) Theoretical growth form of β-hematin viewed along the *a* and *c* axis, respectively. {*h*,*k*,*l*} indices of some faces are indicated. Figure 2. Field emission inlens scanning electron microscopy micrographs of hemozoin purified from (c) *P. falciparum*, (d) *S. mansoni*, (e) *H. columbae*. Representative crystals in (c−e) that strongly resemble the theoretical form are delineated, including one among the horizontally juxtaposed crystals in (d). From ref 28, Copyright (2001) with permission from Elsevier Science.

delineated crystal with sharp faces from the parasite *Plasmodium falciparum* shown in Figure 2c. Other well-formed crystals from the parasite in Figure 2c are clearly visible as ending by an {0,1,1} face, denoted by arrows. The calculated morphology also matches the shapes of the less well-formed crystals from the parasites *Schistosoma mansoni* and *Haemoproteus columbae*, where both the {011} and {001} faces appear to be expressed (Figure 2d,e). The thickness of some β-hematin crystals in Figure 2 may be estimated from the width of the obliquely oriented {010} face, as well as {011}, when projected onto the horizontal {100} plane, as seen for the theoretical growth form by the lighter green shading of the (0$\bar{1}$0) and (0$\bar{1}\bar{1}$) faces in Figure 2a. This procedure has been carried out on four well-shaped specimen crystals in Figure 2c,e each marked with an asterisk, by measuring the width of the sliver of "light" adjacent to the specimen crystal edge parallel to the *c*-axis, which gives a measure of the projected width of the {010} face. We also made use of the projected {011} face on the delineated crystal in Figure 2c.[44] From these values, we derived an average crystal width-to-thickness ratio $w/t = 1.3 (\pm 0.5)$ compared with the corresponding w/t value of the theoretical form, (i.e., E_{att}-{010}/E_{att}{100} in Table 1) = 0.91. The observed ratio is consistent with observation insofar that most of the crystals in Figure 2c−e appear to lie on their {100} faces.

In retrospect, we note that the needle morphology of parasite *P. falciparum* with the obliquely oriented and sharp {011} end face (Figure 2c) would be inconsistent with a crystal structure composed of extended polymer chains.[45]

Effect of Foreign Molecules bound to Crystal Surfaces. It is now well established that minor amounts of a tailor-made additive, which structurally mimics the host molecule present in the solution, may induce dramatic changes in the nucleation properties, growth rate, and morphology of the crystal.[40,41] This effect occurs via selective adsorption of the additive molecule on those surface sites where the modified moiety emerges from the crystal surface, followed by inhibition of regular deposition of oncoming crystal layers. Inhibition of crystal precipitation is best achieved making use of additives designed to retard growth along the fastest-growing directions of the crystal, as observed in the control of crystal polymorphism[46] and the role played by antifreeze proteins in lowering the freezing temperature of the blood serum in fish that inhabit the polar seas.[47] These antifreeze proteins inhibit ice formation as a consequence of stereochemically capping onto the ice surface.

Intercalation of Foreign Molecules within Corrugated Crystal Surfaces. Prior to demonstrating how some antimalarial quinoline drugs can cap onto the fast-growing corrugated {001} surface of the β-hematin crystal, we review examples of inhibition of crystal growth via molecules bound to corrugated faces: The needle crystals of D,L-alanine and the γ-form of glycine grow fastest in aqueous solution at the end face that contains pockets exposing carboxylate oxygen atoms since the water molecules, being weakly occluded within the pockets, do not block solute adsorption therewithin. Growth retardation is achieved through occlusion within the pockets of methanol cosolvent by C−H···O(carboxylate) interactions.[48] In a similar manner, growth of the corrugated crystal surface of α-resorcinol is strongly retarded by water molecules[49,50] bound in the grooves by hydrogen bonds to resorcinol-OH and −CH surface groups.[50,51] Finally, the monolayer crystal structure of cholesteryl L-glutamate on pure water contains corrugated grooves, because of the difference in cross-sectional area of the steroid and glutamate moieties. On an aqueous L-leucine solution, the grooves are occupied by L-leucine that makes both hydrogen bonds and van der Waals contacts with the glutamate moieties.[52]

Adsorption of Chloroquine to the Corrugated {001} Face of β-Hematin. We now examine adsorption of the antimalarial drugs to the weakly developed (001) and (00$\bar{1}$) faces that form at the ends of the β-hematin needle. These two symmetry-related faces are fast growing, as reflected by the highly negative attachment energy ($E_{att} = -101.5$ kcal/mol), which is due to the pronounced {001} crystal surface corrugation and the O−H···O hydrogen bond between the propionic acid groups of neighboring molecules along the $-a$ $+c$ direction. The grooves within the corrugated surface run parallel to the *a*-axis (Figure 3) exposing flexible propionic acid groups, vinyl and methyl groups, as well as aromatic surfaces. Chloroquine, amodiaquine, quinine, and mefloquine (Scheme 1c, d, g, and h), all protonated at the nonprimary exocyclic amine, can each stereochemically cap onto the {001} surface of the β-hematin crystal via (porphyrin)acid-(quinoline)amine salt bridge and still fit snugly on that surface, by intercalation of the quinoline rings between the aromatic groups of the β-hematin molecules, shown for chloroquine in Figure

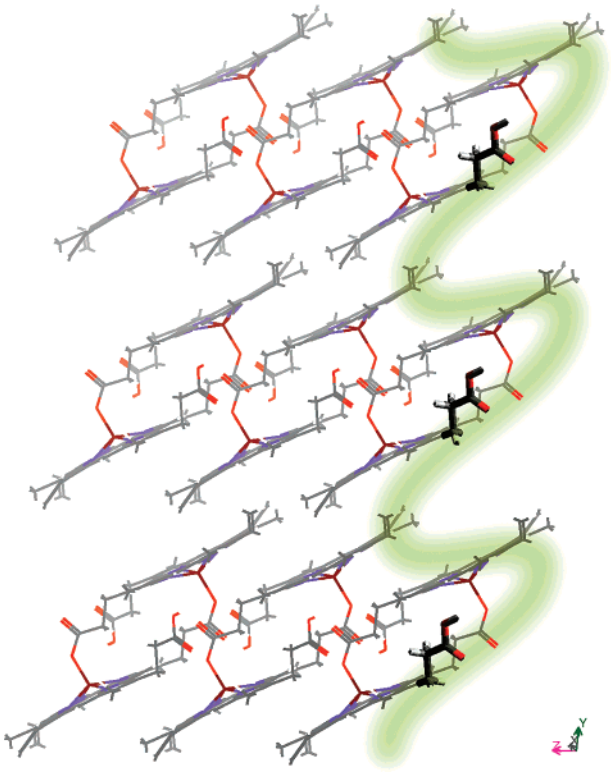

Figure 3. β-Hematin, viewed along the *a*-axis, showing the molecules exposed at the corrugated {001} face, with crevices outlined in green.

Scheme 1. Various Quinolines and Analogues Thereof Reported in the Literature[a]

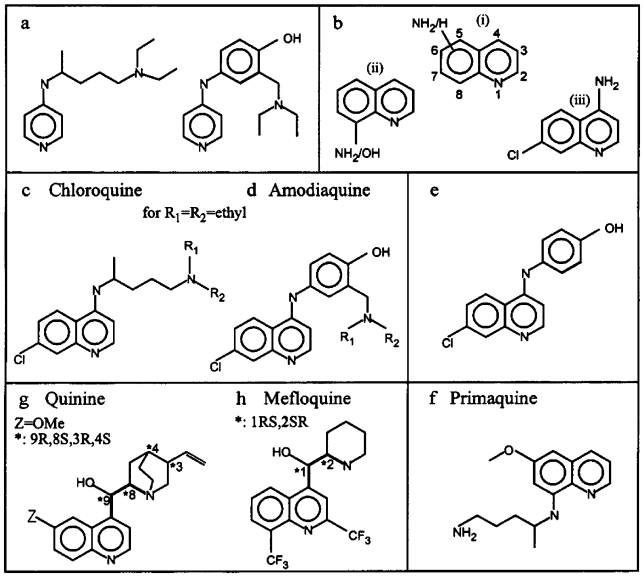

[a] $R_1 = R_2$ = H/ethyl/form a pyrrol ring; R_1 = H and R_2 = ethyl (or R_2 = *tert*-butyl for amodiaquine only), Z = H/OMe.

4. This model is in keeping with early NMR studies on the interaction between chloroquine and hematin in both DMSO and aqueous medium.[69] Chloroquine and amodiaquine also each form an (aromatic)N···HC═C(vinyl) hydrogen bond[53,54] and a CCl···H_3C interaction with the host molecule to help anchor the guest within the crevice (see Figures 4 and 7a).

Quinoline drugs, such as chloroquine, would *not* be able to dock effectively into position at the {001} face,

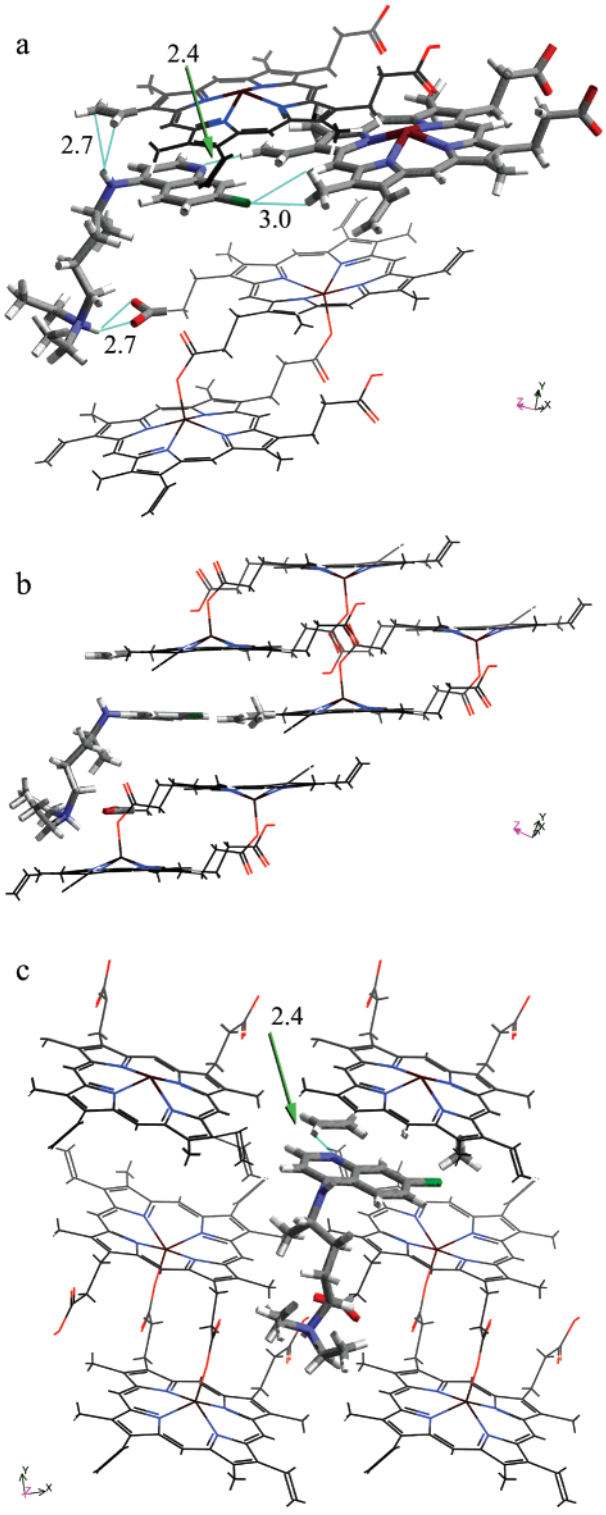

Figure 4. Chloroquine bound to the (001) β-hematin crystal highlighting energetically favorable interactions.[55] The distances are between highlighted atoms. **N···H**C═C 2.4 Å, **Cl···H**$_3$C 3.0 Å, N**H···O**$_2$C 2.7 Å, N**H···C═C**(π-cloud) 2.7 Å. The structure is viewed along (a) a general direction, (b) the *a*-axis, and (c) perpendicular to the {001} face. Chloroquine and some of the groups or molecules of β-hematin are drawn as cylinders.

when protonated also at the aromatic N1 atom: first the (aromatic)N···HC═C(vinyl) hydrogen bond would be precluded and replaced by a longer and unfavorable N−H^+···H−C contact. Second, no neighboring negative counterion would be present. On the other hand, pro-

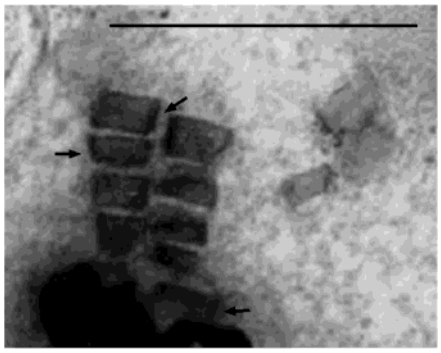

Figure 5. SEM micrograph of digestive vacuole in cultured parasite of *P. falciparum*, where representative arrows point to the more denser regions of the hemozoin crystals, indicating excess location of [^{3}H]chloroquine at their {001} faces. (Bar = 0.5 μm.) From ref 25, Copyright (1996) National Academy of Sciences, USA.

tonation at the aniline N atom (i.e., in chloroquine and amodiaquine) that is exposed to the outside environment may be possible: its unshared electron pair would conjugate only weakly with the aromatic system since the exocyclic chain must twist about the C4−N(aniline) bond to form both the salt bridge with the carboxylate moiety and allow intercalation of the aromatic moiety within the crevice. The protonated (aniline)N−H group would be able to participate in an attractive interaction with the π-system of the neighboring vinyl system[56] (see N**H**···**C**=**C**(π-cloud) contact in Figure 4a). Thus, the precise state of protonation of the bound quinoline molecule may be different from that of the free molecule in the acid vacuole.[57]

Hemozoin crystals within cultured parasites incubated with subinhibitory doses of [^{3}H]chloroquine studied by electron microscope autoradiography shows a pronounced tendency in about seven crystals for drug accumulation in excess at the "end" terminating the longer side of the crystal, which appears to be the {001} face (Figure 5).

Binding of various Quinolines to the {001} Face of β-Hematin. We now examine the proposed binding site at the {001} surface in terms of published results on the antimalarial activity of quinoline drugs, as well as quinoline-related molecules. All of the drugs mentioned have a rigid (aromatic) skeleton, are weak bases, and have a flexible amine moiety.

Most of the reported models regarding the quinoline−hemozoin interaction invoked aromatic π−π interactions, taking note that all of these antimalarial drugs, which inhibit hemozoin crystal growth, incorporate a bicyclic aromatic skeleton. Indeed, the size of the quinoline aromatic moiety is critical for crystal inhibition, as shown by Hawley et al.[21] for the compounds depicted in Scheme 1a, which are about four times less effective as crystallization retardants than either chloroquine or amodiaquine (Scheme 1c,d). This result is clearly in agreement with the model shown in Figure 4; chloroquine should be more tightly bound within the crevice than the compounds shown in Scheme 1a.

The significance of the extended and flexible amine moiety at C4 has been extensively studied during the past decade. When this substituted group is lacking (Scheme 1b(i), (ii)), quinolines do not show evidence of interaction with Fe^{3+}-PPIX, as reported by Egan et al.[27]

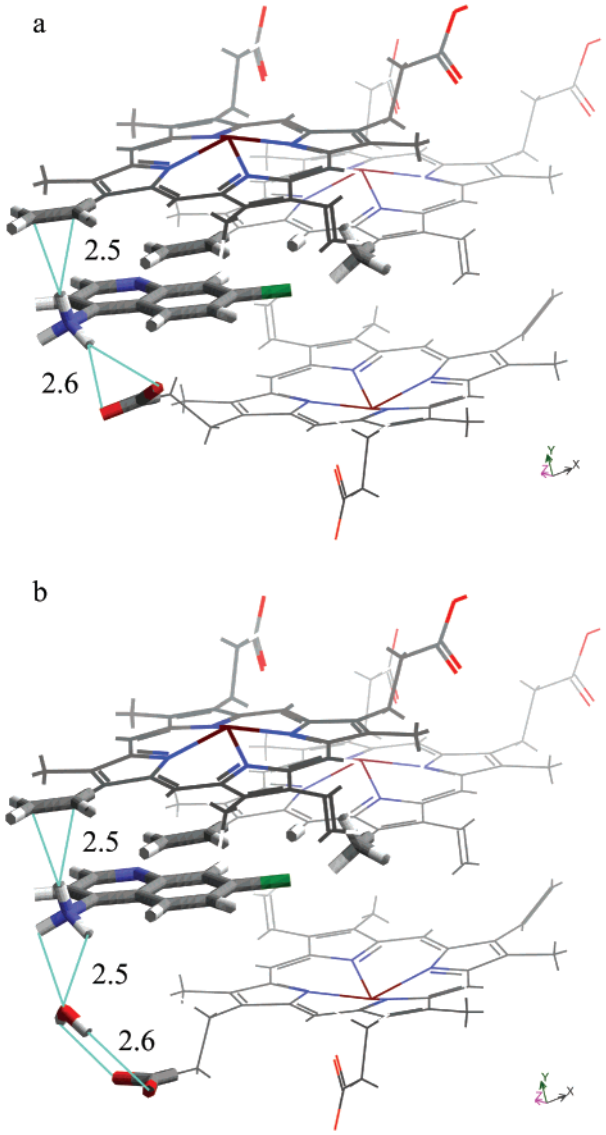

Figure 6. Two possible arrangements of 4-amino-7-chloroquinoline bound to the β-hematin {001} crystal surface, involving: (a) direct linkage between the aniline and carboxylate groups, or (b) via an interleaving water molecule. The distances (in Å) are between highlighted atoms, listed below. (a) N**H**···**C**=**C**(π-cloud) 2.5; N-**H**···**O**$_2$C 2.6 where **N**H···**O**$_2$ = 3.1, (b) N**H**···**C**=**C**(π-cloud) 2.5; N-**H**···**O**H$_2$ 2.5; O-**H$_2$**···**O**$_2$C 2.6.

Admittedly, these drugs can intercalate within the crystal crevice at the {001} face, but would lack either the strong anchoring provided by acid−base pairing or the directed Coulombic interactions discussed previously for chloroquine. These quinoline analogues should readily dissociate from the crystal surface.

The compound 4-amino-7-chloroquinoline (Scheme 1b-(iii)), does inhibit both β-hematin formation and induces in vitro antiplasmodial activity, however, with IC_{50} values[58] about 2 orders of magnitude higher than for chloroquine.[59] The reason for the activity of this compound is its possible association with the flexible propionic acid, either directly by -NH_3^+···^-O_2C- hydrogen bond or via an interleaving water molecule (Figure 6). This acid−base interaction is much weaker than the corresponding bond found for the quinoline drugs (Figures 4 and 7) for the following reasons. Firstly the N-H···O hydrogen bond in the latter systems is shorter

by about 0.5 Å than either the N-H···O or the O-H···O bond involving 4-amino-7-chloroquinoline (Figure 6a,b). Secondly the N-H bond of the quinoline drugs (Figures 4 and 7) tends to lie parallel to the plane of the carboxylate group and directed towards the lone pair electrons of their O atoms to which it is linked by a three-center hydrogen bond. In contrast, the N-H donor of 4-amino-7-chloroquinoline (Figure 6a) tends to be perpendicular to the plane of the carboxylate group, an arrangement less favorable for an attractive Coulomb interaction. The protonated state of the aniline group of 4-amino-7-chloroquinoline is required by the loss of conjugation between the aniline and aromatic systems and the necessity to form an acid-base linkage with the propionic acid moiety.

The importance of nonprimary amine of the exocyclic flexible moiety via both crystal and parasite inhibition tests[60] was demonstrated by Hawley et al.[18,19,21] on various derivatives of chloroquine and amodiaquine (Scheme 1c,d). Amines that are substituted by electron-donating groups (such as hydrocarbons) stabilize positive charge. These ionic structures can form stable salts on interaction with the flexible propionic acid moiety at the binding site.

The quinoline incorporating a hydroxy anilino group instead of a tertiary amine (Scheme 1e) was shown to inhibit β-hematin formation.[21] The phenol OH group may form a hydrogen bond of the type (drug)O−H···OH_2···O(=C−O−Fe) via an interleaving water molecule, akin to amodiaquine (Figure 7a), and the aniline participates in a weak NH_2^+···^-O_2C(acid) interaction with the flexible propionic acid, as described above for 4-amino-7-chloroquinoline (Figure 6). However, the absence of a nonprimary exocyclic amine lowers the degree of the drug's ionic character in the acidic vacuole leading to substantially reduced antiparasitic activity.

The presence of an extended aromatic skeleton and a flexible, nonprimary amine substituent, are a necessary but insufficient condition for effective drug action of the quinolines; their relative positions are also important. Primaquine (Scheme 1f) incorporates an extended exocyclic amine moiety akin to the primary amine derivative of chloroquine (Scheme 1c, $R_1 = R_2 = H$), *however, at the C8 position*. Thus, it is no surprise that primaquine is an inactive drug for the RBC stage of malaria and was found to be a poor crystal growth inhibitor.[21] Its drug−hematin complex of formation (ΔG = −5.9 kcal/mol) is less favorable by ∼1.5 kcal/mol, compared to chloroquine or amodiaquine.[22,61] Although primaquine can bind to the host propionic acid moiety and intercalate within the porphyrin crevice, the pyridine nitrogen emerges from the binding site, precluding formation of the (β-hematin-C=)**C**H···**N**(drug) 3.4 Å hydrogen bond (corresponding C**H**···**N** distance 2.4 Å in Figure 4a,c) that would be replaced by (β-hematin)-**C**H···H**C**(primaquine) contact of ∼4 Å. In addition, the (β-hematin)CH_3···Cl(drug) interaction is also absent. Consequently, primaquine would be less effectively anchored within the crevice compared to all analogues of chloroquine or amodiaquine depicted in Scheme 1c,d.

The antimalarials chloroquine and amodiaquine (Scheme 1c,d) have a drug−hematin complex energy of formation $\Delta G \approx -7.7(\pm 0.4)$ kcal/mol,[22] more favorable by ∼1.5 kcal/mol than that of quinine derivatives and mefloquine (Scheme 1g,h). The former embody a flexible amine chain that extends about 6 Å from the α-substituent of quinoline C4 to the flexible amine, whereas in the latter the corresponding distance is about 3 Å. Furthermore, Ridley et al.[62] performed an in vivo study on the effect of different flexible chain length analogues of chloroquine on β-hematin crystal growth inhibition, making use of chloroquine-sensitive parasites.[63] They report that the drug with a 3 Å chain length induced IC_{50} and ED_{50} values higher by ∼1.5 compared with chloroquine.[58] We may explain the difference in inhibi-

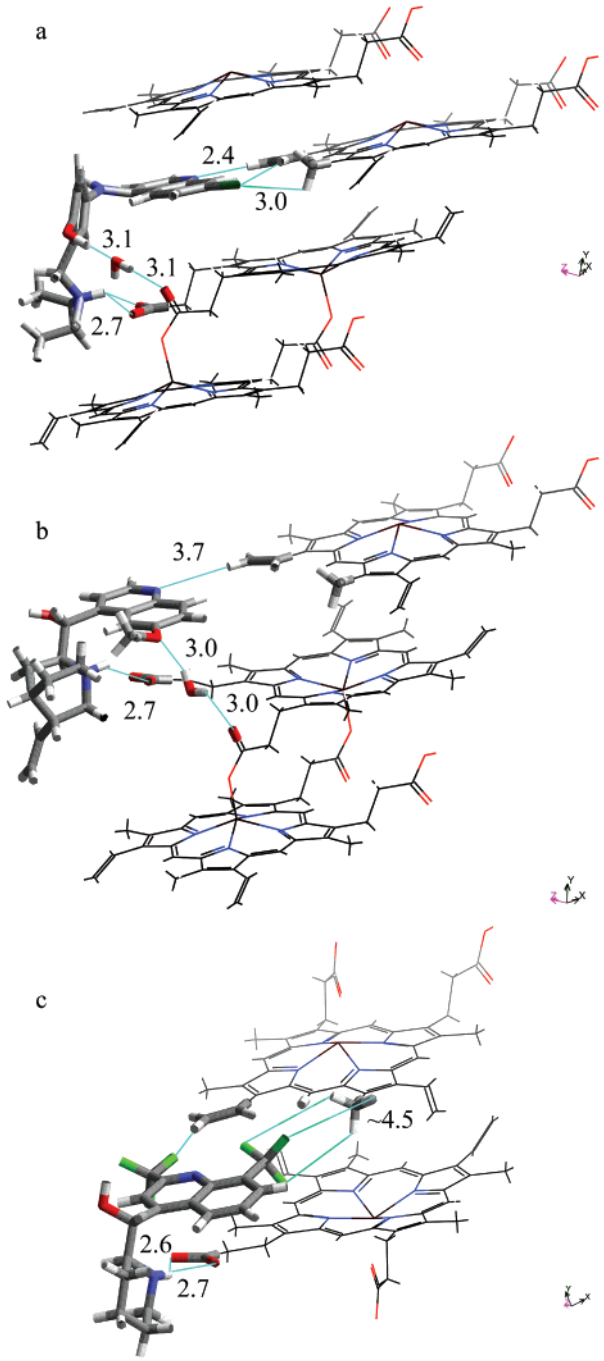

Figure 7. Favorable polar contacts (in Å) between β-hematin at the {001} crystal surface and (a) amodiaquine, (b) quinine, and (c) mefloquine. The distances (in Å) are between highlighted atoms, listed below. (a) **O**-H···**O**H_2···**O**=C−O−Fe 3.1; **N**···**H**-C=C 2.4; **Cl**···**H**$_3$C 3.0; **N**-H···**O**$_2$C 2.7. (b) H_3C-**O**···H-**O**-H···**O**=C−O−Fe 3.0; **N**···**H**-C=C 3.7; **N**-H···**O**$_2$C 2.7. (c) C**F**$_3$···**H**$_3$C 4.5; C-**F**···**H**-C=C 2.6; **N**-H···**O**$_2$C 2.7.

tion of β-hematin crystal growth: the amine at an end of a 6 Å flexible chain interacts more favorably with the host propionic acid moiety, allowing close and attractive (β-hematin)C═CH···N(drug) and (β-hematin)CH_3···Cl-(drug) interactions for chloroquine and amodiaquine (Figures 4 and 7a). Such contacts are forced to be more distant for the shorter chains (quinine and mefloquine in Figure 7b,c). This model is in keeping with the $pK_{association}$ of ~5 for hemozoin−quinoline based drugs[22,27] where the flexible amine "chain length" is ~6 Å, as opposed to ~4 for a length of 3 Å.

The constraints imposed on drug binding by the 3 Å chain length is brought to the fore by the ineffectiveness of the quinine isomer 9S-epiquinine as an antimalarial drug for the RBC stage. Attachment of this molecule to the {001} β-hematin surface in a manner akin to that adopted by quinine (Figure 7b) would induce a gauche configuration between the hydroxyl and tertiary amine bonds.[64] Such an unfavorable conformation can undoubtedly be relieved but at a loss to the acid−base salt bridge.

Other possible interactions not yet mentioned are (drug)O···H−O−H···O(═C−O−Fe) hydrogen bonding quinine to β-hematin via interleaving water, and (mefloquine)CF_3···H_3C(β-hematin)[65] contacts, depicted in Figure 7b,c, respectively.

Several of the different types of quinolines used as antimalarial agents are chiral.[64] The role played by the molecular chirality for inhibiting growth of β-hematin can now be elucidated given its centrosymmetric crystal structure and the faces at which the quinolines may be adsorbed. The crystal surfaces of β-hematin are chiral; thus, the interaction energy between a chiral quinoline with the enantiotopic (001) and (00$\bar{1}$) faces of β-hematin must be different. Therefore, the best strategy would be to use racemic quinolines, other things being equal. This approach has been demonstrated by growth inhibition of centrosymmetric crystals (*R*,*S*)-serine, (*R*,*S*)-*N*-acetylvaline, glycine, and glycylglycine in the presence of chiral tailor-made inhibitors.[66] This point may have some bearing on the relatively low antimalarial activity of quinine, which, being a natural product and of single chirality, perhaps binds more effectively to only one of the two opposite {001} faces, thus allowing the crystal to grow less perturbed at the opposite unaffected face. However, attention must be paid to the particular case, since it would appear from Figure 4 that chloroquine can bind easily to an {001} face in either enantiomeric form.[67]

Comparing crystal growth inhibition of chiral racemic and nonchiral quinolines the latter class appears to have one intrinsic advantage at least from an entropic viewpoint: the molecules can bind to either {001} face, whereas the chiral molecule has to "search" for the appropriate {001} face.

Molecular Isomerism, Binding of Quinolines, Nucleation and Size of β-Hematin Crystals. We may envisage formation of the noncentrosymmetric β-hematin cyclic dimer (Figure 8c) instead of the observed centrosymmetric isomer (Figure 8b) were *one* of the two porphyrin rings of hematin (Fe^{3+}-PPIX, Figure 8a) to react from its opposite face, leading to an interchange of that porphyrin ring's methyl and vinyl groups vis-à-vis the centrosymmetric dimer. The binding

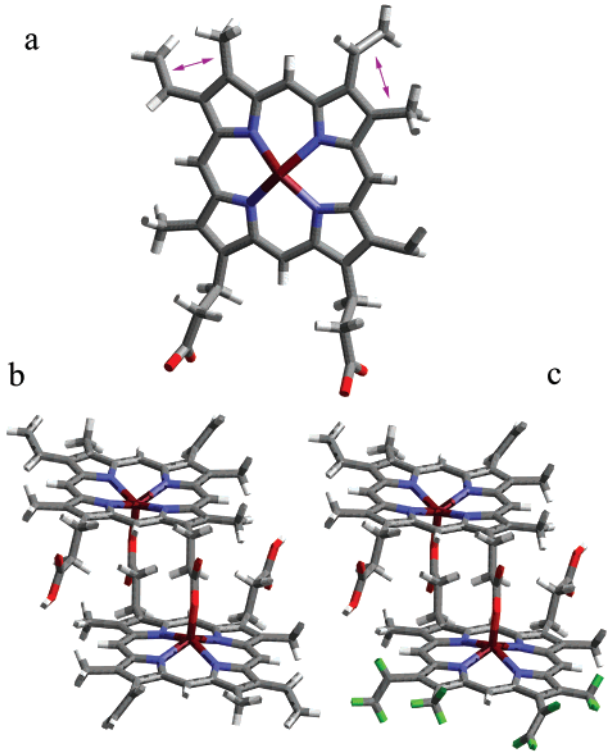

Figure 8. (a) Molecular structure of hematin (Fe^{3+}-PPIX). (b) Centrosymmetric cyclic β-hematin dimer. (c) Noncentrosymmetric dimer, with hydrogens of the "interchanged" groups marked in green. The enantiomer (mirror image) is not shown.

energy of quinolines such as chloroquine and amodiaquine at the {001} face of β-hematin would be less favorable at those surface sites that expose interchanged methyl and vinyl groups of the molecules of the noncentrosymmetric isomer since the (β-hematin)C═CH···N(quinoline skeleton) and (β-hematin)CH_3···Cl-(drug) interactions would be precluded at such sites. Atomic disorder, however, was not detected in the β-hematin crystal structure.[20]

This lack of observable disorder[68] suggests that the surface sites of the growing centrosymmetric crystal may act as a template for β-hematin dimer formation, primarily of the centrosymmetric isomer. The surfaces of triclinic centrosymmetric crystals are chiral on symmetry grounds. We may thus envisage the formation, albeit in small amounts, of the asymmetric dimer at the crystal surface, whose "interchanged" methyl and vinyl groups lie at the {001} crystal surface. Such a "foreign" molecule might behave akin to a "tailor-made" additive[40,41] and retard further crystal growth, leading to submicron to micron-sized crystals, as is invariably observed. Regarding crystal nuclei, in which molecular ordering is generally expected to be low, we may expect that both types of cyclic isomers would be present.

This model is not inconsistent with a recent study by Egan et al.[6] on the mechanism of β-hematin formation in acetate solution. Making use of IR, SEM, and powder X-ray diffraction they concluded that the formation of the β-hematin dimer and crystalline product are essentially simultaneous. They report that β-hematin formation proceeds by rapid precipitation of amorphous (or possible nanocrystalline) hematin, followed by slow conversion into crystalline β-hematin, implying a solid−solid phase transition. A possible drawback to such a

transformation is how to reconcile slow conversion from poorly ordered hematin aggregates to crystalline β-hematin that is fast growing along the *c*-axis and consists of centrosymmetric β-hematin dimers. There is also the related question how quinoline can inhibit growth of the fast growing {001} face of β-hematin, which is being formed from amorphous or nanocrystalline hematin. These difficulties may be circumvented if we assume that the hematin aggregates trigger nucleation of β-hematin, but continued growth follows the templating model described above.

Concluding Remarks

We propose that the fastest-growing {001} crystal faces of β-hematin form the binding sites for the quinoline antimalarials. In this model, the quinoline aromatic ring is interleaved between porphyrin rings within a crevice at the corrugated {001} surface, to which it is further anchored by a salt bridge between the exocyclic amine and a surface-exposed carboxylate group, as well as various adsorbate−host interactions that have a strong Coulombic contribution. The exocyclic amine chain should be sufficiently long and flexible (as in chloroquine) to ensure optimal binding of the distant amine to the host acid moiety, allow appropriate intercalation of the quinoline, and permit the polar interactions alluded to above. The precise state of protonation of the bound quinoline is determined by the interactions with β-hematin and thus may not be the same as the free drug in the acid vacuole that is protonated at both the ring N atom and the exocyclic amine. The doubly protonated state assists in retarding drug diffusion from the acidic vacuole, thus reducing its critical amount for crystal growth inhibition[14,18,19,21] as a result of the bound drug hindering the regular deposition of oncoming {001} molecular layers.

The correlation presented between antimalarial activity of various quinolines and their binding characteristics to the {001} face of β-hematin, albeit qualitative is sufficiently comprehensive to give credence to the model.

A crucial question remains as to the fraction of surface sites that have to be poisoned to inhibit the crystal growth of β-hematin that occurs equally well at the opposite (001) and ($00\bar{1}$) faces for racemic or nonchiral quinolines according to the model presented. Inhibition would be more efficient were the drug stereochemically also bound to other faces, for example {100}, at which the propionic acid groups are exposed, albeit with an oblique orientation. We may therefore envisage more effective crystal growth inhibitors that bind onto the corrugated {001} face to two or more surface sites related by 12 Å translation along the *a*-axis. Such molecules may also be able to bind effectively to neighboring propionic acid groups on the {100} face, and thus strongly inhibit crystal growth along both the *a* and *c* axes, unlike drugs used to date that contain only one nonprimary amine function. Several types of quinoline dimers incorporating the amine function, not designed according to the above principle, have shown substantial crystal and parasitic growth inhibition.[22,70−72] It is of interest that the quinoline antimalarials used to date could not take advantage of the exposed carbonyl O═C(−O−Fe) functional group on the {001} face for direct hydrogen bonding, but only via interleaving water as invoked above for quinine and amodiaquine. This drawback may be remedied by future design.

The role played by quinoline chirality for inhibiting growth of β-hematin has been touched upon. It should now be possible to take advantage of the chiral shape of the enantiotopic {001} faces of β-hematin for the design of more effective racemic quinolines.

The possibility was raised that the growing hemozoin crystal surfaces act as a template for formation of β-hematin centrosymmetric cyclic dimers. Furthermore, the asymmetric dimer might dock onto the growing crystal surface, leading to crystal growth inhibition, and thus account for the formation of the micron-size crystals. The extent of occlusion of the asymmetric cyclic dimer within the centrosymmetric β-hematin crystal, if at all present in observable quantities, may be determined by a low-temperature X-ray diffraction study. This possibility should also be taken into account with regard to drug design.

Methods

The crystal structure of β-hematin was extracted from the atomic coordinates reported by Pagola et al.[20] To compute the crystal attachment energies, the lattice energy of the crystal structure was minimized using the Cerius2[42] software package, having adjusting the lengths of the C−H bonds to a standard value. The atomic potential parameters included both dispersion and Coulomb contributions. The crystal attachment energies were computed via Cerius2 from which the theoretical growth form was derived, applying the Hartman-Perdok approach.[30−32]

The molecular structure of the various quinolines was constructed using the Cerius2 software package.[42] The intramolecular energies of the various quinolines were initially minimized using universal 1.02 force field. The quinoline conformation and docking surface site position and orientation were adjusted manually to yield acceptable interatomic contact distances.

Acknowledgment. We thank Prof. Michael McBride for enlightening discussions, and Dr. Isabelle Weissbuch for her helpful comments on reviewing the manuscript. We are particularly grateful to Prof. Meir Lahav, for only by virtue of a long collaboration on the effect of tailor-made additives and solvent on nucleation growth and morphology of crystals was it possible to carry out this work.

References

(1) Bouland, P. B. *Drug Resistance in Malaria*; World Health Organization: Switzerland, 2001.
(2) Kirk, K. *Physiol. Rev.* **2001**, *81*, 495−537.
(3) Olliaro, P. *Pharmacol. Ther.* **2001**, *89*, 207−219.
(4) Ziegler, J.; Linck, R.; Wright, D. W. *Curr. Med. Chem.* **2001**, *8*, 171−189.
(5) Ginsburg, H. http://sites.huji.ac.il/malaria/, 2002.
(6) Egan, T. J.; Mavuso, W. W.; Ncokazi, K. K. *Biochemistry* **2001**, *40*, 204−213.
(7) Hempelmann, E.; Egan, T. J. *Trends Parasitol.* **2002**, *18*, 11.
(8) Lowenstam, H. A.; Weiner, S. *On Biomineralization*; Oxford University Press: New York, 1989.
(9) Wellems, T. E.; Plowe, C. V. *J. Inf. Dis.* **2001**, *184*, 770−776.
(10) Bray, P. G.; Mungthin, M.; Ridley, R. G.; Ward, S. A. *Mol. Pharmacol.* **1998**, *54*, 170−179.
(11) Ginsburg, H.; Geary, T. G. *Biochem. Pharmacol.* **1987**, *36*, 1567−1576. and citations therein.
(12) Ginssburg, H.; Nissany, E.; Kruglak, M. *Biochem. Pharmacol.* **1989**, *38*, 2645−2654.

(13) Gray, T. G.; Divo, A. D.; Jensen, J. B.; Zangwill, M.; Ginssburg, H. *Biochem. Pharmacol.* **1990**, *40*, 685−691.

(14) In chloroquine $pK_{a1} = 8.1$ is assigned to the ring nitrogen and the $pK_{a2} = 10.2$ to the side chain tertiary amine nitrogen (ref 12). The pK_{a3} of the secondary aniline amine nitrogen is estimated at 5.0 (refs 73−75). Calculating the extent of ionization of weak base in the two pH environments using the Henderson-Hasselblach equation for the various amines of chloroquine, we obtain for physiological pH = 7.4: 0.4% (5.0), 83.4% (8.1), 99.8% (10.2), and in the acidic vacuole pH = 4.8: 61.3% (5.0), 99.9% (8.1), and 100% (10.2).

(15) Yayon, A.; Cabantchik, Z. I.; Ginsburg, H. *Proc. Natl. Acad. Sci. U.S.A.* **1985**, *82*, 2784−2788.

(16) Gary, T. G.; Jensen, J. B.; Ginssburg, H. *Biochem. Pharmacol.* **1986**, *35*, 3805−3812.

(17) Bray, P. G.; Boulter, M. K.; Ritchie, G. Y.; Ward, S. A. *Mol. Biochem. Parasitol.* **1994**, *63*, 87−94.

(18) Hawley, S. R.; Bray, P. G.; Park, B. K.; Ward, S. A. *Mol. Biochem. Parasitol.* **1996**, *80*, 15−25.

(19) Hawley, S. R.; Bray, P. G.; O'Neill, P. M.; Park, K.; Ward, S. A. *Biochem. Pharmacol.* **1996**, *52*, 723−733.

(20) Pagola, S.; Stephens, P. W.; Bohle, D. S.; Kosar, A. D.; Madsen, S. K. *Nature* **2000**, *404*, 307.

(21) Hawley, S. R.; Bray, P. G.; Mungthin, M.; Atkinson, J. D.; O'Neill, P. M.; Ward, S. A. *Antimicrob. Agents Chemother.* **1998**, *42*, 682−686.

(22) Dorn, A.; Vippagunta, S. R.; Matile, H.; Jaquet, C.; Vennerstrom, J. L.; Ridley, R. G. *Biochem. Pharmacol.* **1998**, *55*, 727−736.

(23) Macomber, P. B.; Sprinz, H.; Tousimis, A. J. *Nature* **1967**, *214*, 937.

(24) Sullivan, D. J. J.; Matile, H.; Ridley, R. G.; Goldberg, D. E. *J. Biol. Chem.* **1998**, *273*, 31103−31107.

(25) Sullivan, D. J. J.; Y., G. I.; Russell, D. G.; Goldberg, D. E. *Proc. Natl. Acad. Sci. U.S.A.* **1996**, *93*, 11865−11870.

(26) The reported cell constants are $a = 12.20$ Å, $b = 14.68$ Å, $c = 8.04$ Å, $\alpha = 90.2°$, $\beta = 96.8°$, $\gamma = 97.9°$, space group $P\bar{1}$.

(27) Egan, T. J.; Mavuso, W. W.; Ross, D. C.; Marques, H. M. *J. Inorg. Biochem.* **1997**, *68*, 137−145.

(28) Chen, M. M.; Shi, L.; Sullivan, D. J. J. *Mol., Biochem. Parasitol.* **2001**, *113*, 1.

(29) Egan, T. J.; Ross, D. C.; Adams, P. A. *FEBS Lett.* **1994**, *352*, 54−57.

(30) Hartman, P.; Perdok, W. G. *Acta Crystallogr.* **1955**, *8*, 49.

(31) Hartman, P.; Perdok, W. G. *Acta Crystallogr.* **1955**, *8*, 525.

(32) Hartman, P. *Crystal Growth: An Introduction*; North-Holland Publishing Co.: Amsterdam, 1973.

(33) Hartman, P.; Benema, P. *J. Cryst. Growth* **1980**, *49*, 145.

(34) Berkovitch-Yellin, Z. *J. Am. Chem. Soc.* **1985**, *107*, 3375.

(35) Weissbuch, I.; Shimon, L. J. W.; Addadi, L.; Berkovitch-Yellin, Z.; Lahav, M.; Leiserowitz, L. *Israel J. Chem.* **1985**, *25*, 353.

(36) Weissbuch, I.; Berkovitch-Yellin, Z.; Leiserowitz, L.; Lahav, M. *Isr. J. Chem.* **1985**, *25*, 362.

(37) Boek, E. S.; Feil, D.; Briels, W. J.; Bennema, P. *J. Cryst. Growth* **1991**, *114*, 389−410.

(38) Docherty, R.; Meenan, P. In *Molecular Modeling Applications in Crystallization*; Myerson, A. S., Ed.; Cambridge University Press: 1999; p 106.

(39) Woensdregt, C. F. *Faraday Discuss.* **1993**, *95*, 97.

(40) Weissbuch, I.; Addadi, L.; Lahav, M.; Leiserowitz, L. *Science* **1991**, *253*, 637−645.

(41) Weissbuch, I.; Popovitz-Biro, R.; Lahav, M.; Leiserowitz, L. *Acta Crystallogr. B* **1995**, *51*, 115−148.

(42) Cerius2 v. 4.5, Accelrys Inc., San Diego, CA, 2000.

(43) {*h*, *k*, *l*} denotes both (*h*, *k*, *l*) and (−*h*, −*k*, −*l*) faces.

(44) To reduce errors due to the possibility that the specimen crystals may not lie exactly parallel to the plane of the {100} face we had made use of crystals with different azimuths, as well as the projected thickness of the {011} face.

(45) Extended polymer chains would most likely lie parallel to the long axis of the crystal, in this case the *c*-axis, even though such a crystal would grow by side-to-side juxtaposition of the polymer chains. Since such chains will not be of the same length their ends cannot form a smooth obliquely oriented {011} face.

(46) Weissbuch, I.; Leiserowitz, L.; Lahav, M. *Adv. Mater.* **1994**, *6*, 953−956.

(47) Knight, C. A.; Cheng, C. C.; Devries, A. L. *Biophys. J.* **1991**, *59*, 409−418.

(48) Shimon, L. J. W.; Vaida, M.; Addadi, L.; Lahav, M.; Leiserowitz, L. *J. Am. Chem. Soc.* **1990**, *112*, 6215.

(49) Davey, R. J.; Milisavljevic, B.; Bourne, J. R. *J. Phys. Chem.* **1988**, *92*, 2032.

(50) Wireko, F. C.; Shimon, L. J. W.; Frolow, F.; Berkovitch-Yellin, Z.; Lahav, M.; Leiserowitz, L. *J. Phys. Chem.* **1987**, *91*, 472.

(51) Hussain, M.; Anwar, J. *J. Am. Chem. Soc.* **1999**, *121*, 8583−8591.

(52) Alonso, C.; Eliash, R.; Jensen, T. R.; Kjaer, K.; Lahav, M.; Leiserowitz, L. *J. Am. Chem. Soc.* **2001**, *123*, 10105−10106.

(53) Berkovitch-Yellin, Z.; Leiserowitz, L. *Acta Crystallogr.* **1984**, *B40*, 159.

(54) Bernstein, J.; Etter, M. C.; Leiserowitz, L. *Structure Correlation*; Buergi, H.-B. and Dunitz, J. D., Ed.; VCH: Weinheim, 1994; Vol. 2.

(55) The energy of the C═C−H···N hydrogen bond should be in the same range as the C═C−H···O(carbonyl) bond (ref 54), which is about 2 kcal/mol. The N−H···C═C interaction should be in the same energy range as the C≡C−H···C−≡C bond that was found to be similar to the C≡C−H···O(carbonyl) interaction (ref 53). We do not have any quantitative data on the CH_3···Cl interaction, but since the Cl substituent is electronegative and the methyl H atom has a net positive charge we may assume an attractive Coulomb interaction. The energy of the moderately strong three-center $N-H^{+}\cdots{}^{-}O_2$(carboxylate) hydrogen bond, which occurs in several zwitterionic α-amino acid crystal structures, must be no less than 6 kcal/mol.

(56) Steiner, T. *Angew. Chem., Int. Ed.* **2002**, *41*, 48−76. In this review OH···C═C interactions were referred to, rather than NH···C═C.

(57) It is noteworthy that the γ-crystalline form of glycine, which is in a zwitterionic state, is obtained from an aqueous solution of glycine made acidic with acetic acid or basic with ammonium hydroxide (ref 76).

(58) IC_{50} (inhibitory concentration 50) is the concentration of a compound needed to reduce population growth of organisms by 50% in vitro. The ED_{50} (effective dose 50) is the amount of material required to produce a specified effect in 50% of an animal population.

(59) Egan, T. J.; Hunter, R.; Kaschula, C. H.; Marques, H. M.; Misplon, A.; Walden, J. *J. Med. Chem.* **2000**, *43*, 283−291.

(60) The IC_{50} values (ref 58) for drug-mediated crystal inhibition in vitro experiments was usually higher than for in-vivo experiments (using chloroquine sensitive parasites). This difference may be attributed to the ability of the molecule to accumulate within the food vacuole, increasing its local concentration at the target site.

(61) Thermodynamic parameters for various quinolines were also calculated for neutral pH ∼ 7.5 by Egan et al. (refs 27 and 77) in 40% DMSO, while Dorn et al. (ref 22) measured at pH ∼ 6.5 in water, with similar results.

(62) Ridley, R. G.; Hofheinz, W.; Matile, H.; Aquet, C.; Dorn, A.; Masciardi, R.; Jolidon, S.; Richter, W. F.; Guenzi, A.; Girometta, M.-A.; Urwyler, H.; Huber, W.; Thaithong, S.; Peters, W. *Antimicrob. Agent. Chemother.* **1996**, *40*, 1846−1854.

(63) De et al. (ref 78) made an elaborate study on various chloroquine analogues with different flexible amine lengths, against chloroquine sensitive vs resistant parasites, but which showed a small scatter in IC_{50} values.

(64) Warhurst, D. C. *Biochem. Pharmacol.* **1981**, *30*, 3323−3327.

(65) Jacquemain, D.; Wolf, S. G.; Levieiller, F.; Frolow, F.; Eisenstein, M.; Lahav, M.; Leiserowitz, L. *J. Am. Chem. Soc.* **1992**, *114*, 9983−9989. In this reference the net charge of −0.14e units on F atoms was determined experimentally from a deformation electron density analysis of low-temperature X-ray diffraction data. The net charge on the H atom is about +0.06 e units.

(66) Addadi, L.; Berkovitch-Yellin, Z.; Weissbuch, I.; Lahav, M.; Leiserowitz, L. *Topics in Stereochemistry*; J. Wiley & Sons: New York, 1986; Vol. 16.

(67) Chloroquine in either enantiomeric form can bind almost equally well to an {001} face according to Figure 4. The opposite enantiomer at the (001) surface site, obtained by interchanging the CH_3 and H groups attached to the asymmetric C atom, does not appear to embody poor intramolecular contacts, nor introduce a noticeable change in intermolecular contacts.
(68) After the Rietveld refinement of the crystal structure that involved about 480 Bragg reflections (ref 20), the authors report no significant electron densities in a Fourier difference map; the densities ranged between −0.10 to +0.09 $e^-/Å^3$. However, whether the X-ray powder diffraction analysis can reveal atomic disorder between the vinyl and methyl groups as low as 5−10% is a moot point.
(69) Moreau, S.; Perly, B.; Biguet, J. *Biochimie* **1982**, *64*, 1015−1025.
(70) Raynes, K.; Foley, M.; Tilley, L.; Deaddy, L. W. *Biochem. Pharmacol.* **1996**, *52*, 551−559.
(71) Ridley, R. G.; Matile, H.; Aquet, C.; Dorn, A.; Hofheinz, W.; Leupin, W.; Masciardi, R.; Theil, F.-P.; Richter, W. F.; Girometta, M.-A.; Guenzi, A.; Urwyler, H.; Gocke, E.; Potthast, J.-M.; Csato, M.; Thomas, A.; Peters, W. *Antimicrob. Agent. Chemother.* **1997**, *41*, 677−686.
(72) Ismail, F. M. d.; Dascombe, M. J.; Carr, P.; Merette, S. A. M.; Rouault, P. *J. Pharm. Pharmacol.* **1998**, *50*.
(73) Streitwieser, A.; Heathcock, C. H.; Kosower, E. M. *Introduction to Organic Chemistry*; 4th ed.; Prentice Hall: Upper Saddle River, NJ, 1998.
(74) Bordwell, F. G. *Table of pK_a*, http://www.chem.wisc.edu/areas/reich/pkatable/index.htm, **2002**.
(75) Evans, D. *Table of pK_a* Harvard, http://daeiris.harvard.edu/DavidEvans.html, **1997**.
(76) Iitaka, Y. *Acta Crystallogr.* **1961**, *14*, 1−10.
(77) Egan, T. J.; Hempelmann, E.; Mavuso, W. W. *J. Inorg. Biochem.* **1999**, *73*, 101−107.
(78) De, D.; Krogstad, F. M.; Byers, L. D.; Krogstad, D. J. *J. Med. Chem.* **1998**, *41*, 4918−4926.

CG025550I